THE JOURNAL OF BIOLOGICAL CHEMISTRY
Vol. 279, No. 48, Issue of November 26, pp. 50391–50400, 2004
Printed in U.S.A.

Structural and Biochemical Identification of a Novel Bacterial Oxidoreductase*

Received for publication, August 4, 2004, and in revised form, August 30, 2004
Published, JBC Papers in Press, September 7, 2004, DOI 10.1074/jbc.M408876200

Lodovica Loschi‡, Stephen J. Brokx§, Tanya L. Hills‡, Glen Zhang§, Michela G. Bertero‡¶, Andrew L. Lovering‡‖, Joel H. Weiner§, and Natalie C. J. Strynadka‡ ‡‡**

From the ‡Department of Biochemistry, University of British Columbia, Vancouver British Columbia V6T 1Z3 and §Canadian Institutes of Health Research Membrane Protein Research Group, Department of Biochemistry, University of Alberta, Edmonton, Alberta T6G 2H7, Canada

By using a bioinformatics screen of the *Escherichia coli* genome for potential molybdenum-containing enzymes, we have identified a novel oxidoreductase conserved in the majority of Gram-negative bacteria. The identified operon encodes for a proposed heterodimer, YedYZ in *Escherichia coli*, consisting of a soluble catalytic subunit termed YedY, which is likely anchored to the membrane by a heme-containing trans-membrane subunit termed YedZ. YedY is uniquely characterized by the presence of one molybdenum molybdopterin not conjugated by an additional nucleotide, and it represents the only molybdoenzyme isolated from *E. coli* characterized by the presence of this cofactor form. We have further characterized the catalytic subunit YedY in both the molybdenum- and tungsten-substituted forms by using crystallographic analysis. YedY is very distinct in overall architecture from all known bacterial reductases but does show some similarity with the catalytic domain of the eukaryotic chicken liver sulfite oxidase. However, the strictly conserved residues involved in the metal coordination sphere and in the substrate binding pocket of YedY are strikingly different from that of chicken liver sulfite oxidase, suggesting a catalytic activity more in keeping with a reductase than that of a sulfite oxidase. Preliminary kinetic analysis of YedY with a variety of substrates supports our proposal that YedY and its many orthologues may represent a new type of membrane-associated bacterial reductase.

Molybdenum-coordinating enzymes fall within the broad class of enzymes associated with redox metabolic functions in prokaryotic and eukaryotic cells. The structurally characterized enzymes can be roughly grouped into three separate families (the bacterial/eukaryotic xanthine oxidase family, the eukaryotic sulfite oxidase family, and the bacterial Me_2SO reductase family), each distinctive with respect to active site structure and the type of reaction they catalyze (1). The family of xanthine oxidases contains 1 eq of a pterin cofactor coordinated to the molybdenum metal with the typical pentavalent, approximately octahedral coordination sphere in the oxidized state completed not by any side chains from the enzyme but rather by a double-bonded sulfur atom, a double-bonded oxygen atom, and an oxygen atom with a single bond (2). Sulfite oxidases have 1 eq of a pterin cofactor with the molybdenum coordinated by a cysteine ligand from the enzyme and two oxo groups (3, 4). Kappler *et al.* (5) described the spectroscopic and enzymologic characterization of a member of the sulfite oxidase family from *Thiobacillus novellus*, and they showed that the enzyme contains a molybdopterin-type cofactor, but no structural data are available for bacterial sulfite oxidase family members to verify the nature of the cofactor or overall architecture of this enzyme. The Me_2SO reductase family is diverse in both structure and function, but all members have 2 eq of the pterin cofactor, and the molybdenum coordination sphere is usually completed by a single oxo group and a sixth ligand that can be a serine as in Me_2SO reductase (6), a cysteine in nitrate reductase (7), a selenocysteine in formate dehydrogenase H (8), and a hydroxy and/or water molecule in arsenite oxidase (9). Recently, Bertero *et al.* (10) reported the first nitrate reductase structure with the molybdenum ion coordinated by an aspartic acid. Molybdoenzymes are generally conserved across the family to which they belong, and the sequence identity becomes even more significant when only the residues involved in the active site are considered.

In this paper, we present the crystal structure of YedY from *Escherichia coli* at 2.5-Å resolution. The gene encoding for YedY was identified in the *E. coli* genome (11) sequence as a novel molybdoenzyme, and it was predicted to have a molybdopterin-type cofactor based on sequence similarity with known molybdopterin-containing structures. Our structural and biochemical analysis indicates that YedY constitutes the catalytic subunit of a novel membrane-associated complex found in the majority of Gram-negative bacteria. YedY is the only molybdoenzyme isolated from *E. coli* with the molybdopterin-type cofactor, and it represents the first structural characterization of this form of cofactor in prokaryotes and of a member of the bacterial sulfite oxidase family. Even though the overall fold of YedY is surprisingly similar to domain II of the eukaryotic chicken sulfite oxidase (CSO)[1] and *Arabidopsis*

* This work was supported by the National Institutes of Health, the Canadian Institutes of Health Research, and the Howard Hughes Medical Institute. The costs of publication of this article were defrayed in part by the payment of page charges. This article must therefore be hereby marked "*advertisement*" in accordance with 18 U.S.C. Section 1734 solely to indicate this fact.

The atomic coordinates and structure factors (codes 1XDQ and 1XDY) have been deposited in the Protein Data Bank, Research Collaboratory for Structural Bioinformatics, Rutgers University, New Brunswick, NJ (http://www.rcsb.org/).

¶ Canadian Institutes of Health Research fellow.
‖ Michael Smith Foundation for Health Research postdoctoral fellow.
** Hold the Canada Research Chair in Membrane Biochemistry.
‡‡ Canadian Institutes of Health Research Scientist and Howard Hughes Medical Institute International Scholar. To whom correspondence should be addressed: Dept. of Biochemistry and Molecular Biology, University of British Columbia, 2146 Health Sciences Mall, Vancouver, British Columbia V6T 1Z3, Canada. Tel.: 604-822-0789; Fax: 604-822-5227; E-mail: natalie@byron.biochem.ubc.ca.

[1] The abbreviations used are: CSO, chicken liver sulfite oxidase; PSO, *Arabidopsis thaliana* sulfite oxidase; PDB, Protein Data Bank; MOPS, 4-morpholinepropanesulfonic acid; TMAO, trimethylamine *N*-oxide; Moco, molybdenum cofactor.

thaliana sulfite oxidase (PSO), our structural data indicate that the active site of YedY shows striking differences, which suggest a catalytic activity more in keeping with a reductase rather than a sulfite oxidase enzyme. Those findings are supported by preliminary kinetic data with a variety of substrates.

EXPERIMENTAL PROCEDURES

Expression and Purification of YedY—The complete *E. coli* genome sequence (11) was examined for potential novel molybdoenzymes, based on sequence similarity with known molybdopterin-containing proteins. One unknown gene identified in this search was *yedY* (b1971).

The plasmid pMSYZ3 contains His_6-tagged YedY (YedYHis6) and native YedZ cloned as described,[2] behind the *ptac* promoter. The protein was expressed in *E. coli* strain JM109 transformed with the pMSYZ3 plasmid. The cells were grown in Terrific Broth (12) with the addition of 0.003% (w/v) metal ion mixture (13), except the $(NH_4)_6Mo_7O_{24}\cdot 4H_2O$ was replaced with 1 mM $NaMoO_4$. The growth was achieved aerobically at 30 °C in 1.5 liters of media in a 4-liter flask, and expression was induced with 0.1 mM isopropyl β-D-thiogalactoside at A_{600} ~0.8. The cells were incubated for a further 12 h before harvesting. In order to incorporate tungsten in the cofactor, cells were grown in media in which the 1 mM $NaMoO_4$ was substituted with 10 mM $Na_2WO_4\cdot 2H_2O$. The cell pellets were washed in 100 mM MOPS, 5 mM EDTA, pH 7.0, resuspended in MOPS buffer containing 0.4 mM phenylmethylsulfonyl fluoride, and broken open by sonication. In order to assess the presence of YedYHis6 in the periplasm, the periplasmic fraction was isolated by osmotic shock, following the procedure described elsewhere (14, 15). In both cases the supernatant was separated from the cell debris by ultracentrifugation at 150,000 × *g* at 4 °C with a Beckman L8-M Ultracentrifuge (rotor type 60Ti) and contained soluble YedYHis6. The supernatant was then applied to a Chelating Sepharose Fast Flow resin (Amersham Biosciences) pre-equilibrated with 20 mM MOPS, pH 7.0, 0.5 M NaCl, and eluted with a gradient of 0–50 mM histidine. The fractions containing YedYHis6 were further purified by anion exchange chromatography on a 10/10 MonoQ column (Amersham Biosciences). YedYHis6 containing the molybdenum cofactor did not bind to the column; after concentration it was applied to a 10/30 Superdex 200 size exclusion chromatography column (Amersham Biosciences) equilibrated with crystallization buffer (20 mM MOPS, pH 7.0, 150 mM NaCl). One peak containing YedYHis6 was obtained that corresponds to monomeric YedYHis6. YedYHis6 with incorporated tungsten was purified following the same procedure. Selenomethionine-substituted YedYHis6 was expressed in the same *E. coli* strain as the native protein. Cells were grown as described previously (16), and the protein was purified by following the same protocol as for wild-type YedYHis6. The protein samples were concentrated to a final concentration of 15 mg/ml and stored at −80 °C in 50-μl aliquots after flash-freezing in liquid nitrogen.

As expected due to the presence of a twin arginine translocation sequence leader, wild-type YedYHis6, tungsten YedYHis6, and selenomethionyl YedYHis6 were expressed in the periplasmic domain of *E. coli*. Whether they were purified from total soluble protein or specifically from the periplasmic fraction, we obtained the proteins in a homogenous and fully processed form (298 amino acids, molecular mass of 33,580 Da), as confirmed by electrospray mass spectrometry and N-terminal sequencing (DLLSWF). The yield for wild-type YedYHis6 was ~0.1 mg of protein per g of cells. The complete substitution of Met residues in the selenomethionyl derivative was confirmed by electrospray mass spectrometry. Static light scattering experiments indicated that the protein is monodisperse and is present as monomer in solution. The incorporation of molybdenum and tungsten cofactors was confirmed by UV-visible spectrophotometry (data not shown).

Mass Spectrometry—Homogeneity of fully processed YedY was checked through electrospray mass spectrometry, as well as for incorporation of selenomethionine. Mass spectra were recorded on a PESciex API 300 triple quadrupole mass spectrometer (Sciex, Thornhill, Ontario, Canada) equipped with an ion spray source.

Static Light Scattering—Static light scattering experiments were done at 25 °C on a Superdex 200 column (Amersham Biosciences) using 20 mM MOPS, pH 7.0, 150 mM NaCl. Refractive index and Mini-dawn light scattering detectors (Wyatt Technology) were calibrated using bovine serum albumin (Sigma).

Kinetic Analysis—YedY sulfite oxidase activity was monitored as described previously, by using either *Saccharomyces cerevisiae* cytochrome *c* (17) or ferricyanide (18) as electron acceptor, and varying the concentration of sulfite between 2.5 and 400 μM. Steady-state kinetic measurements were performed aerobically at 25 °C using a 1.0-cm light path cuvette and a final sample volume of 1.0 ml, and the increasing absorbance at 550 nm was followed. YedY reductase activity was monitored as previously described (19). Substrate-dependent oxidation of the electron donor, reduced benzyl viologen (BVH^+), was monitored at 570 nm. For open cuvette (nonstoppered) assays, using degassed MOPS buffer, benzyl viologen was used at a final concentration of 0.22 mM (ϵ of $BVH^+ = 7.8 \times 10^3$ liters mol^{-1} cm^{-1}) and sodium dithionite at a concentration of 0.63 mM. The final assay volume was kept constant, with the ordered addition of benzyl viologen, substrate, and enzyme. Each data point was the average of duplicate values, and kinetic data of k_{cat} and K_m were determined by Hanes plot.

Crystallization—Native YedYHis6 crystals were grown at 18 °C by vapor diffusion methods by using 0.5 μl of protein solution and 0.5 μl of well solution per drop. Crystals of the orthorhombic space group $I2_12_12_1$ with dimensions a = 110.73 Å, b = 164.45 Å, and c = 180.95 Å were obtained in 1.4 M Li_2SO_4, 0.1 M triethanolamine, pH 7.3, using 15 mg/ml protein solution. Crystals typically reached their final size of ~0.2 × 0.3 × 0.2 mm^3 within typically 4 days and diffracted x-rays to 2.5 Å by using synchrotron radiation. Selenomethionyl derivative crystals were obtained under the same conditions as native YedY, using 15 mg/ml protein solution, and grew in the same crystal form. Native YedYHis6 and selenomethionine YedYHis6 crystals were predicted to have five molecules per asymmetric unit, based on unit cell dimensions and self-rotation function; the Matthews coefficient is V_M = 2.5 $Å^3$ Da^{-1}, which corresponds to a solvent content of 49.4%. Tungsten-substituted YedYHis6 crystallized in the monoclinic $P2_1$ space group, with a = 84.84 Å, b = 177.55 Å, c = 104. 22 Å, and β = 109.74°. They were grown using a 15 mg/ml protein solution and well solution consisting of 0.1 M magnesium formate, 15% polyethylene glycol 3350, in a 1:1 ratio. Tungsten-substituted YedYHis6 crystals were predicted to have 10 molecules per asymmetric unit based on unit cell dimensions and self-rotation function; the Matthews coefficient is V_M = 2.2 $Å^3$ Da^{-1}, which corresponds to a solvent content of 43.6%.

Data Collection and Structure Determination—All data collection was carried out at 100 K. Crystals were transferred into solutions of the cryo-protectant (containing concentrations of 1 M urea, 1.25 M LiCl, and 5% glycerol for native YedY and the selenomethionine derivative, and 1 M urea, 0.1 M magnesium formate, 20% polyethylene glycol 3350 for tungsten YedY).

Data sets SEMET and NAT (Table I) were collected at beamline 8.3.1 at the Advanced Light Source, Berkeley, CA, on an ADSC Q210 detector at a wavelength of 0.979651 Å. Both data sets were processed with DENZO (20) and scaled with SCALEPACK. Data set WNAT (Table I) was collected at beamline 8.2.2 at the Advanced Light Source, on an ADSC Q315 detector, at a wavelength of 1.54 Å. Collection at the beamline maximum intensity was impossible because of immediate crystal decay. The data set was processed with MOSFLM and scaled with SCALA (21).

Selenium sites were determined by using Shake and Bake, version 2.0 (22), and refined by SHARP (23). Twenty three out of 25 sites in the asymmetric unit were identified and were subsequently used as input for SOLVE (24) to obtain the remaining two sites and to calculate phases to a resolution of 4 Å (resulting figure of merit 0.41 for all data from 40.0 to 4.0 Å). The initial map was improved using density modification and NCS averaging with RESOLVE (25), which was also used to extend the phases to 2.5 Å resolution against the data set NAT, and to determine the NCS relationships between the five monomers (final figure of merit 0.48 for all data from 40.0 to 2.5 Å). An initial model was built using XtalView (26), consisting of 250 residues of one monomer, which was used as a search model in MolRep (21) for the remaining four monomers. The model was refined against data set NAT at 2.5 Å resolution and incorporating NCS averaging in CNS (27). The weight of the NCS restraints used was 300 at the beginning and relaxed to 50 in the final round of refinement. Iterative rounds of model building and refinement with CNS were performed.

The initial model for tungsten-substituted YedY was obtained by molecular replacement with MolRep (21) using the pentamer of native YedY as search model, and it was refined against data set WNAT at 2.2 Å resolution in CNS (27). No NCS restraints were incorporated during the rounds of refinement. Statistics for data collection, phasing, and refinement are summarized in Table I. The molybdenum cofactor, putative urea molecule, and the coordinating oxo and water groups were all refined at full occupancy (1.0). Test refinement trials to substantiate the two additional non-protein coordinating atoms of the molybdenum were done by using combinations of both oxo and water molecules (two

[2] S. J. Brokx, R. A. Rothery, G. Zhang, and J. H. Weiner, manuscript in preparation.

TABLE I
Data collection, phasing, and refinement statistics

Data collection	Compound		
	Selenomethionyl (SEMET)	Native (NAT)	Tungsten (WNAT)
Space group	$I2_12_12_1$	$I2_12_12_1$	$P2_1$
Unit cell dimensions (Å)			
a	110.728	110.345	84.842
b	164.449	165.064	177.513
c	180.950	181.447	104.214
Wavelength (Å)	0.979651	0.979651	1.54
Resolution range (Å)	50.0–3.3	50.0–2.55	50–2.2
Unique reflections	48,051	51,827	146,127
Average multiplicity	7.0	3.9	3.4
Completeness (%)[a]	99.3 (97.7)	96.5 (82.1)	99.3 (98.7)
$\langle I/\sigma I\rangle$[a]	15.2 (4.7)	16.3 (2.2)	10.2 (2.4)
R_{merge}[a,b]	0.116 (0.403)	0.069 (0.496)	0.131 (0.424)
Figure of merit			
after SHARP centric/acentric		0.16/0.39	
after SOLVE		0.41	
after RESOLVE		0.44	
Refinement			
Compound	NAT		WNAT
Resolution range (Å)	40.0–2.55		40.0–2.2
R_{work}[c]	0.230		0.225
R_{free}[d]	0.274		0.258
Average *B*-factor (Å^2)			
Overall	56.9		56.8
Water	36.8		36.3
Root mean square deviation			
Bond length (Å)	0.011		0.008
Angles (°)	1.7		1.6

[a] Values in parenthesis correspond to the highest resolution shell.
[b] $R_{merge} = S|(I_{hkl}) - \langle I\rangle|/S(I_{hkl})$, where I_{hkl} is the integrated intensity of a given reflection.
[c] $R_{work} = (S|F_{obs} - F_{calc}|)/(SF_{obs})$, where F_{obs} and F_{calc} are observed and calculated structure factors.
[d] 5% of reflections were excluded from the refinement to calculate R_{free}.

waters, one oxo/one water, two oxos). Based on temperature factor, distance, and lack of positive or negative residual density, we found that, at this resolution, one coordinating atom (OM2) could be unambiguously identified as an oxo group (distance of ~1.7 Å, thermal parameters of ~35 Å^2, and no residual density after refinement), but the second coordinating atom, which also interacts with the bound urea, could be refined equally well as a water molecule coordinating the ligand and also hydrogen bonding to the urea or as an oxo coordinating the molybdenum with a close hydrogen bond to an adjacent water molecule which in turn hydrogen-bonds to the urea. Higher resolution data or a substrate-bound complex will be required to distinguish these two possibilities for this coordinating atom. The final refined model shows good stereochemistry with 85.3 and 14.2% of residues in the most favorable region and in the additional allowed region of the Ramachandran plot (28), respectively, for NAT, and 85.0% and 14.6% for WNAT. Residues 19–257 and 264–285 of each monomer could be built in the structure.

RESULTS AND DISCUSSION

Identification of a Putative Novel Oxidoreductase, YedYZ—The determination of the *E. coli* genome sequence (11), containing a large number of genes of unknown function, has touched off renewed searches for genes encoding possible novel and important functions. In this study, we examined the *E. coli* genome for potential novel molybdoenzymes. One unknown gene identified in this search was *yedY* (b1971). In addition the presence of a twin arginine signal peptide was of interest. YedY is a soluble periplasmic protein with a twin arginine signal peptide for processing by the twin arginine translocation (Tat)/membrane targeting translocation (MTT) system (29, 30), with a processed molecular mass of 33,580 Da. It is proposed to be the catalytic subunit of the heterodimer, based on our sequence analysis suggesting the presence of ligands for one redox center, namely molybdopterin. Sequence analysis and topology mapping of YedZ predicts six transmembrane segments (31), suggesting a potential role in anchoring YedY to the bacterial membrane. Sequence analysis and the optical spectrum of the reduced *versus* oxidized membranes (enriched with YedZ) (32) are characteristic of a *b*-type heme, with an α component at 559 nm (data not shown), indicating that YedZ is likely similar to cytochrome b_{559} and in the overall electron transfer pathway with YedY. Further analysis of the biochemical interaction between YedY and YedZ will be required to confirm that YedZ is the redox partner for YedY. Most intriguingly, YedYZ orthologues are found in a wide variety of bacteria, primarily Gram-negative, including important clinical pathogens of humans, animals, and plants (Fig. 1), namely *Erwinia carotovora*, *Brucella melitensis,* and *Campylobacter jejuni*. The members of this broad family of proteins are highly similar in primary sequence (typically >50% identity with YedY) and are entirely uncharacterized in terms of structure and function. YedY and its orthologues align poorly with other well characterized molybdoenzymes, including the sulfite oxidases, Me_2SO reductases, and xanthine oxidases, with no conservation of the key catalytic groups found in these systems.

Overall Architecture—We have determined the structure of YedY using MAD phasing from incorporated selenomethionine. YedY is a spherical molecule of mixed $\alpha + \beta$ structure with overall dimensions 50 × 45 × 40 Å and an accessible surface area of ~11,800 Å^2 (Fig. 2*A*). The overall fold of YedY consists of 10 β-strands, organized into two β-sheets, and 12 α-helices. Both β-sheets are mixed, and they are located on opposite sides of the molybdenum cofactor (Moco). The C-terminal β-sheet centers on the two longest β-strands (β3 and β4) of the domain, which form a long and twisted β-hairpin. The α-helices are predominantly short and exposed to bulk solvent. α5 and α6 are located before and after the long β-hairpin of the domain, respectively, and they form a hydrophobic surface region located on the opposite side of the Moco (Fig. 3*B*). YedY shares no structural features with the bacterial molybdenum cofactor containing enzymes of the families Me_2SO reductase (7) or xanthine oxidase (33) (Fig. 2, *A*, *C*, and *D*).

A comparison of YedY with the currently available protein

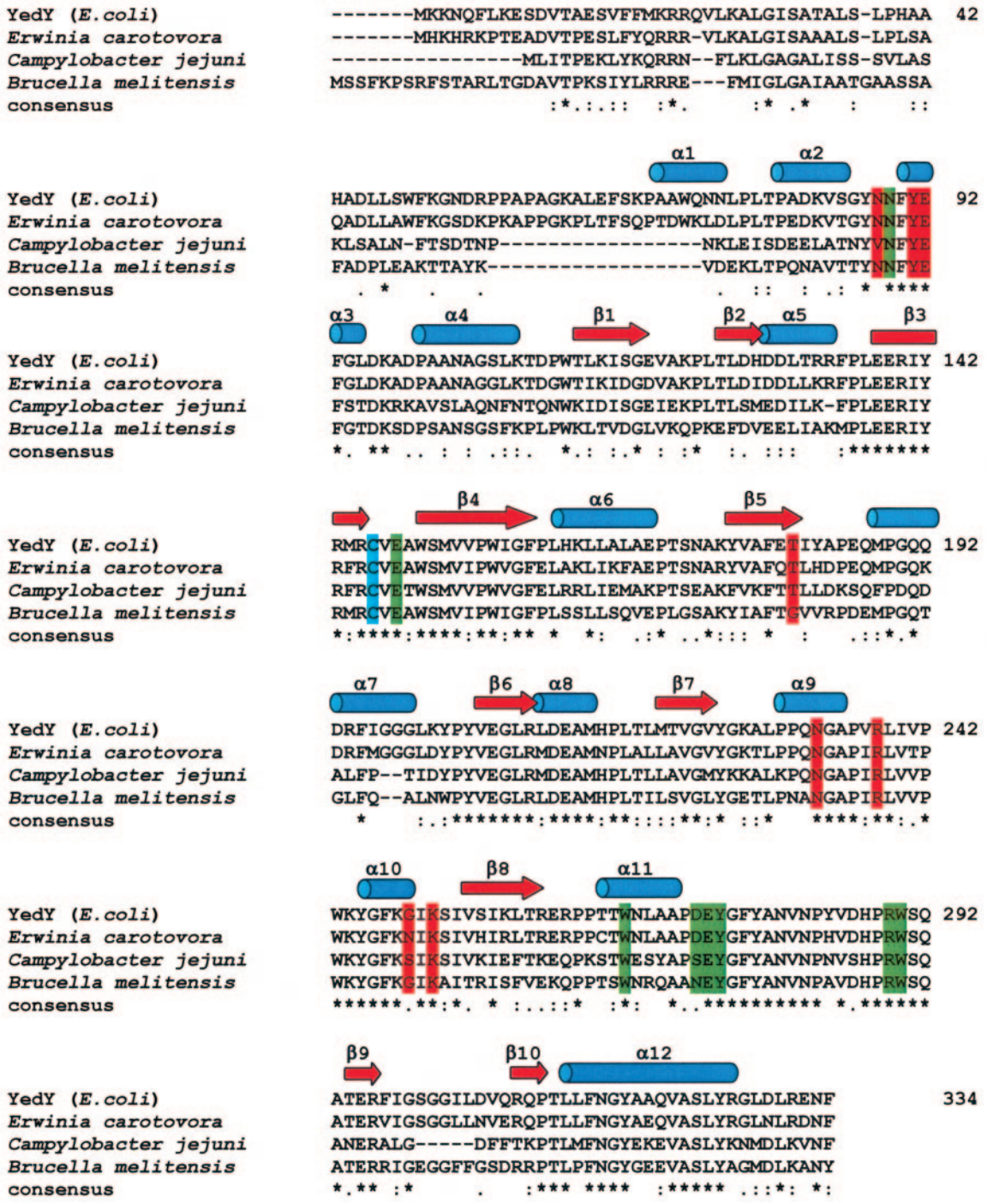

FIG. 1. **Sequence alignment of the YedY family.** YedY and orthologues proteins from *E. carotovora*, *C. jejuni,* and *B. melitensis* are compared. Secondary structural elements, determined with PROMOTIF (49), are indicated. Gaps in the sequence are denoted by *dashes*, and identical residues are denoted by *asterisks* in the consensus line. Residues involved in molybdenum coordination, pterin cofactor coordination, and in the active-site cavity are labeled as follows: *cyan* for the coordinating cysteine, *green* for residues involved in active-site cavity, and *red* for residues coordinating the pterin cofactor via hydrogen bonds through main chain and side chain atoms.

structures in the PDB (analyzed using the program DALI (34)) shows that despite relatively low sequence identity (18%), the fold of YedY is most similar to that of CSO, with a significant Z score of 16.1. Superimposition of the two structures (3) shows the single YedY domain is similar to only domain II of CSO (the Moco containing domain) (Fig. 2*B*), with a root mean square deviation of 1.7 Å for 157 common C-α atoms (secondary structure matching server, EMBL-EBI), but lacks analogous structures to the two additional CSO domains, one of which is responsible for dimerization and the other of which is responsible for the binding of heme. Although not detected in DALI, a second published sulfite oxidase, that of the plant *A. thaliana* (PSO) (4) also shows significant structural similarity with YedY (root mean square deviation of 2.21 Å for 165 common C-α atoms). Again, YedY matches only with the Moco containing domain from PSO and has no structural counterpart to the dimerization domain of the plant enzyme.

There are five YedY monomers in the asymmetric unit of the native enzyme crystal related by a noncrystallographic 5-fold axis (Fig. 3*A*). The model consists of residues 18–283. For all subunits both the N and C termini (including the noncleavable His tag) were disordered, and the electron density map for the

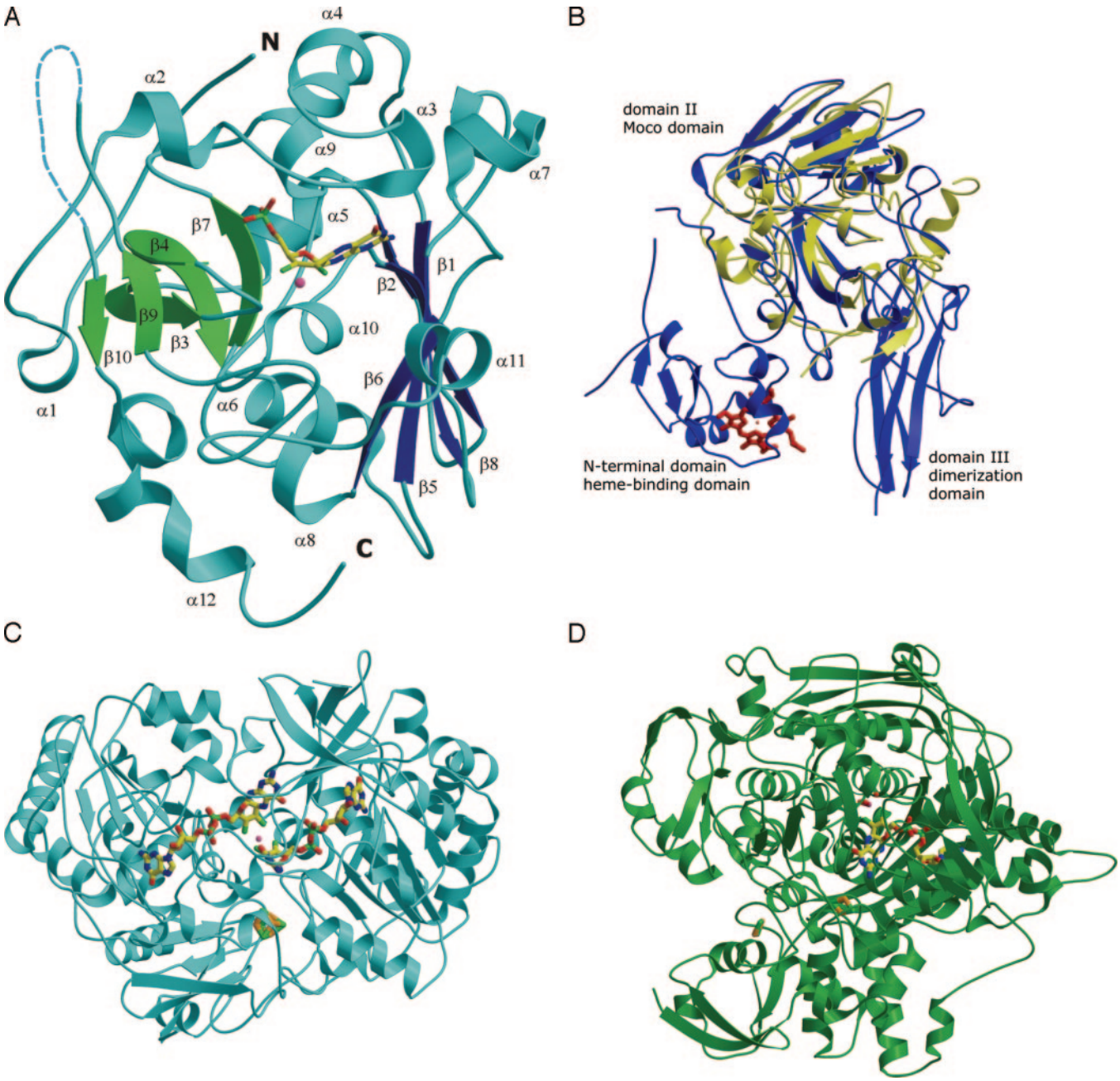

FIG. 2. *A*, a ribbon representation of the YedY monomer. The two β-sheets and the α-helices are in *blue* (N-terminal β-sheet), *green* (C-terminal β-sheet), and *cyan* (α-helices). The Moco is in a *ball* and *stick* representation with the molybdenum ion in *pink*. Secondary structure elements are labeled. *B*, C-α superimposition of YedY (*yellow*) and CSO (*blue*; PDB code 1SOX). *C*, overall structure of the dissimilatory nitrate reductase from *Desulfovibrio desulfuricans* ATCC27774 (PDB code 2NAP) representing the family of Me_2SO reductases. The molybdenum cofactor and the [4Fe-4S] cluster are in *ball* and *stick*. *D*, overall structure of the aldehyde oxidoreductase from *D. gigas* representing the family of xanthine oxidases (PDB code 1VLB). The molybdenum cofactor and the two [2Fe-2S] clusters are in *ball-and-stick*. The figures were generated with MOLSCRIPT (50).

loop between residues 257 and 263 was poorly defined. All subunits are highly similar with a range of root mean square deviations of 0.06–0.18 Å resulting from the superposition of 264 common C-α atoms. The pentamer forms a large ring-like structure with an inner channel of 34 Å, and each subunit contacts only two of the other four subunits of the pentamer. The distances between the cofactors are ~38 Å between the closest subunits and ~61 Å with the second neighbor, precluding inter-subunit electron transfer. Most intriguingly, all five subunits are topologically aligned in a similar manner, such that the Moco containing regions all lie on the same face. In addition, a conserved hydrophobic region of each monomer, localized opposite to the Moco containing domain (Fig. 3*B*), align together to form an extended hydrophobic surface that could play a role in membrane association and/or interaction with its redox partner YedZ. However, the relevance of the observed oligomerization of YedY is uncertain. The buried surface area between each pair of monomers in the pentamer is ~1132 $Å^2$, consistent with physiologically relevant oligomers (35), but the interaction surface lacks the significant hydrophobic or hydrogen-bonded interactions that typically mediate oligomeric states. There are only four direct hydrogen bonds, and no significant hydrophobic interactions at the oligomeric interface in YedY. In comparison, CSO and PSO dimers are characterized by distinct dimerization domains that provide 1573 and 1690 $Å^2$ of buried surface, respectively, and the presence of 20–30 intersubunit direct hydrogen bonds (3, 4). YedY is also observed as a monomer in solution at protein concentrations of

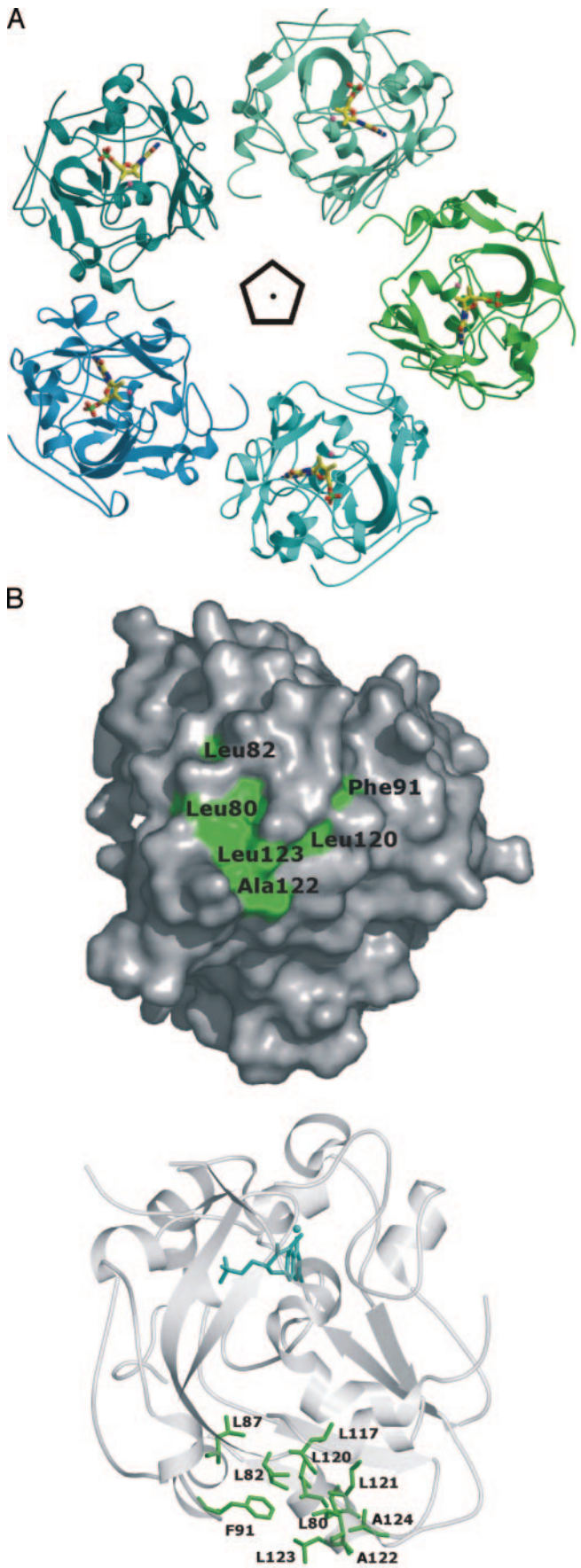

FIG. 3. **Overall architecture of YedY.** *A*, ribbon representation of the YedY pentamer. The five monomers are color-coded differentially. The 5-fold axis perpendicular to the plane is indicated. The molybdenum cofactors are in *ball* and *stick* representation with the molybdenum ions in *pink*. The figure was generated with MOLSCRIPT (50). *B*, *top*, hydrophobic surface map of the monomer showing the presence of a hydrophobic surface region (*green*) on the opposite site of the Moco and *ball-and-stick* representation (*bottom*) of conserved residues forming the hydrophobic patch. The *top figure* was generated with PyMol (51), and the *bottom figure* was generated with MOLSCRIPT (50).

15 mg/ml, using static light scattering analysis (data not shown).

The Active Site of YedY—Molybdenum-containing enzymes are divided into three families, depending on their distinctive active-site structure and on the type of reaction catalyzed (1). Among the structures available, only xanthine oxidase and xanthine dehydrogenase from bovine milk (2) and sulfite oxidases from chicken liver (3) and from *A. thaliana* (4) are characterized by the presence of a single molybdopterin not conjugated by nucleotide. Xanthine oxidase and dehydrogenase have an $LMo^{VI}OS(OH)$ core in the oxidized state, with 1 eq of the pterin cofactor (designated L) coordinated to the metal and a double-bonded sulfur atom, a double-bonded oxygen atom, and an oxygen atom with a single bond completing the coordination sphere (2). The aldehyde oxidoreductase from *Desulfovibrio gigas*, the only structurally characterized representative of a bacterial enzyme from the xanthine oxidase family, has a molybdenum cofactor similar to the enzyme from cow's milk but is conjugated by a cytosine nucleotide (36). In sulfite oxidases the (oxidized) metal center has a single equivalent of the pterin cofactor, but as part of an $LMo^{VI}O_2$(S-Cys) core, with a cysteine ligand provided by the polypeptide and two oxo groups completing the coordination of the metal ion (3, 4).

The active site of YedY possesses several novel features that have no precedent in other characterized bacterial electron transfer proteins. The molybdenum cofactor consists of a single molybdopterin that is localized such that the molybdenum atom is ~16 Å from the enzyme surface. The cofactor is relatively buried within the enzyme active site, although the molybdenum ion itself is partially exposed to bulk solvent. As in all structurally characterized molybdenum enzymes (2–4, 6, 7, 33, 37, 38), the pterin is comprised of a tricyclic ring system with the pyran ring fused to the pyrazine ring of the pterin. The molybdopterin is not conjugated by an additional nucleotide, and YedY represents the only structure of a prokaryotic enzyme with a molybdopterin-type cofactor.

The molybdenum cofactor forms numerous hydrogen bonds with main chain and side chain atoms in YedY, which are strictly conserved across the family of bacterial YedY-related proteins (Figs. 1 and 4). The pterin interacts with the protein by seven direct hydrogen bonds involving Tyr-47 (N-O4), Glu-48 (Oϵ1-N3, Oϵ2-N2), Thr-137 (Oγ1-N2), Lys-207 (N-N1), Gly-205 (O-N8), Arg-194 (Nη2-O3′), and the terminal phosphate group is stabilized by six additional hydrogen bonds formed by Arg-194 (Nη2-O4′, Nη2-O2P), Asn-189 (Nδ2-O2P), Lys-207 (Nζ-O1P, Nζ-O2P), and Asn-44 (Nδ2-O1P). These observed interactions that anchor the molybdenum cofactor tightly to the enzyme are distinct from those observed in the eukaryotic oxidase enzymes that bind a similar Moco (3, 4). In YedY, the molybdenum ion is coordinated by three sulfur ligands, two contributed from the dithiolene sulfurs of the molybdopterin with a Mo-S distance of 2.4 Å. The third sulfur ligand is Sγ of Cys-102 (numbering refers to the processed YedY, starting at Asp-1) at a distance of 2.4 Å. Although at the present resolution of our model it is not possible to absolutely identify the chemical nature of additional atoms bound to the molybdenum ion (there being precedent for both bound sulfur and oxygen atoms), test refinements of combinations of both oxo and water molecules for coordination of the molybdenum ion were done. One oxo group (OM2) fit the electron density

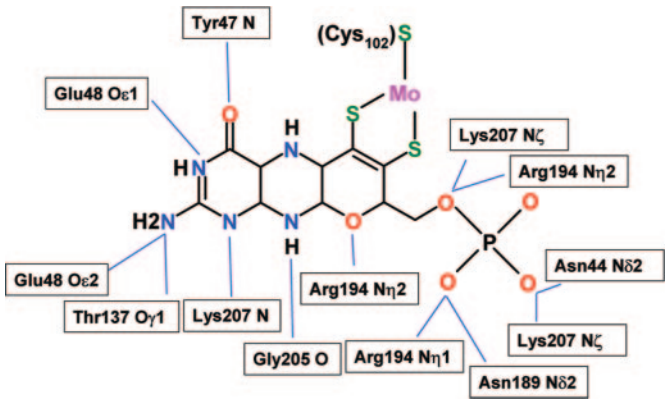

FIG. 4. **Schematic representation of the interactions between Moco and YedY.** Hydrogen bonds are indicated by *blue lines.*

unambiguously with refined distances of 1.6–1.8 Å) for the five molecules of the asymmetric unit (see "Experimental Procedures"). However, due to the presence of adjacent electron density from a bound molecule (proposed to be urea from our crystallization buffer, see below), we cannot distinguish unambiguously the position of the second coordinating atom as it can be refined with similar parameters at the typical length for an oxo group (1.6–1.8 Å and with an intervening water between it and the bound urea) or for a water molecule (2.1–2.4 Å and a direct hydrogen bond to bound urea). Both these scenarios have been observed previously in the eukaryotic molybdopterin enzymes, with two oxo groups coordinating the molybdenum in the *A. thaliana* sulfite oxidase (4) at distances of ~1.7 Å, and one oxo group and one water molecule adjacent to the bound substrate sulfate ion coordinating the molybdenum ion at distances of 1.7 and 2.2 Å, respectively, in the chicken sulfate oxidase structure (3). In YedY, the Nδ2 of the conserved Asn-45 is within hydrogen bonding distance from one of the oxo groups, and the main chain amide nitrogens of Val-103, Gly-202, and Phe-203 are within hydrogen bonding distance from the second coordinating oxygen atom.

An open pocket adjacent to the Moco represents the only likely area for substrate binding, barring a major conformational rearrangement (Fig. 6*A*). The proposed pocket is formed by Asn-45, Glu-104, Tyr-47, Tyr-231, Trp-223, and Trp-246. Most intriguingly, residual electron density at 2.0σ, which remains unaccounted for by protein or bulk solvent, could account for a possible substrate or substrate mimic bound at the active site (Fig. 5*A*). The planar, extended density lies near the second coordinating atom of the molybdenum coordination sphere and is within hydrogen bonding distance to the hydroxyl groups of Tyr-47 and Tyr-231. In order to address the nature of the bound molecule, we systematically refined various components of appropriate size that were known to be contained within our crystallization and cryo-protectant mixtures. Correspondingly, in our YedY structure the additional electron density map was modeled with water/hydroxo and sulfate, MOPS, and water/hydroxo and urea. The anionic sulfate ion and MOPS molecule (with characteristic tetrahedral sulfate geometry) were not optimally fit into the flat density and refined poorly with temperature factors above 100 Å^2. Conversely, the planar urea molecule fit the density optimally and refined with a thermal factor of 50 Å^2 at full occupancy. Despite the fact that YedY was crystallized under conditions similar to chicken liver sulfite oxidase (3) with 1.4 M Li_2SO_4 as precipitant, there is no evidence for sulfite binding in the active site (see below). In contrast, in the CSO structure (3) water/hydroxo ligand and sulfate were reliably modeled in an analogous site, representing a reduced form of the enzyme with bound product.

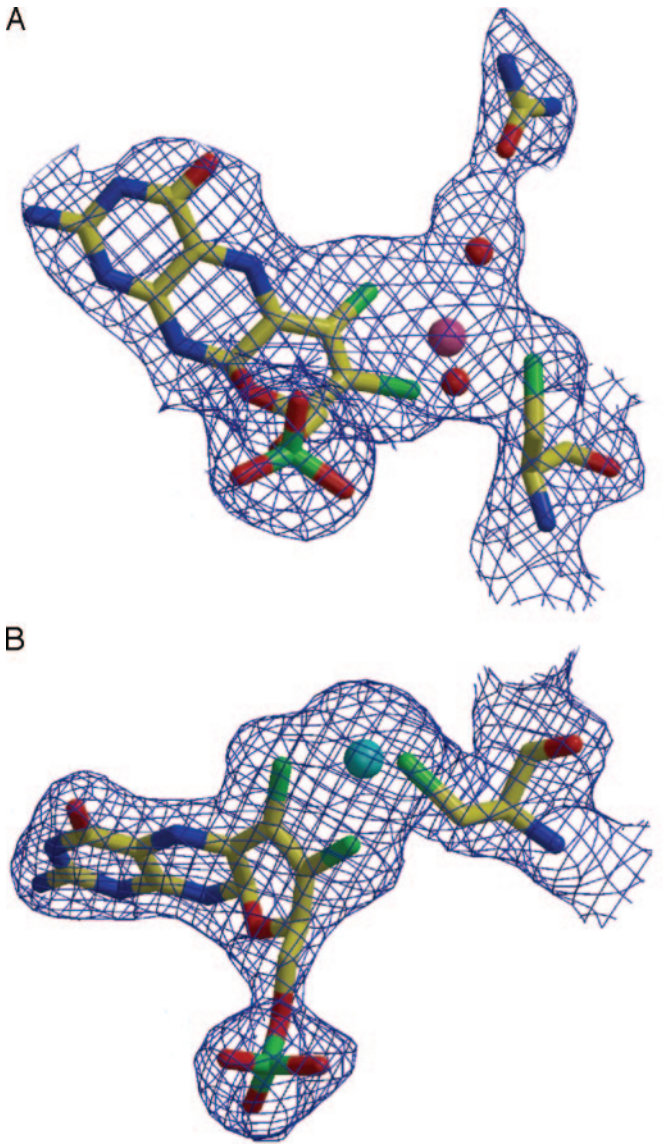

FIG. 5. **The substrate binding pocket.** *A*, the $2F_o - F_c$ electron density map of native YedY contoured at 1σ. The figure shows the presence of additional electron density adjacent to the molybdenum ion, modeled with water/hydroxo and urea. The figure was generated with Bobscript (50). *B*, similar view of tungsten-substituted YedY showing the absence of bound substrate. Tungsten is in *cyan*.

Comparison of the substrate binding pockets of YedY and CSO reveals striking structural differences that explain the disparity in substrate preference between these two enzymes (Fig. 6, *A* and *B*). In particular, YedY lacks the cluster of strictly conserved basic residues characteristic of CSO and other eukaryotic sulfite oxidases (Arg-138, Arg-190, and Arg-450 in CSO). These arginines form a dense complimentary electrostatic network with the bound sulfate ion in the CSO structure (3). Most interestingly, mutation to a glutamine residue at one of these positions in the human sulfite oxidase (Arg-160, the equivalent to Arg-138 in CSO) has been shown to lead to a lethal sulfite oxidase deficiency that has been identified in several infants worldwide (39–41). Subsequent work has shown that the presence of an arginine residue at this position is not only crucial for the formation of the positively charged sulfite-binding site but is also essential for an efficient intramolecular electron transfer between the reduced heme [Fe(II)] and the oxidized molybdenum [Mo(VI)] (42). In YedY, Asn-45 occupies the analogous position to Arg-138 in CSO, and the side chains of Glu-230, Tyr-231, and Trp-246 in YedY

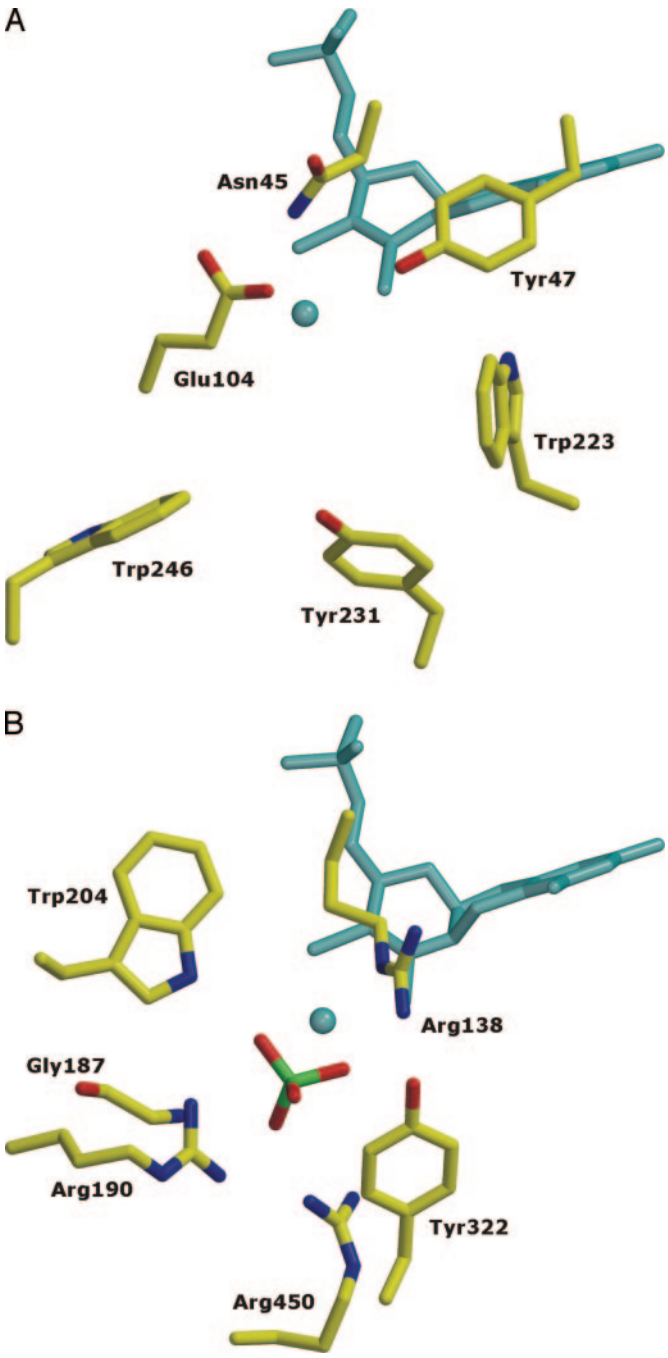

FIG. 6. ***Ball-and-stick* representation comparing key features of the active sites of YedY (*A*) and CSO (*B*).** The figures were generated with MOLSCRIPT (50). Moco and Mo are in *cyan*.

occupy the same area as Arg-190 and Arg-450 in CSO. Moreover, the carboxylate side chain of a glutamic acid residue (Glu-104) presides directly within the substrate binding pocket of YedY, clearly generating an electrostatic clash with putative anions such as sulfate and sulfite (this position is a glycine in CSO, with the main chain nitrogen coordinating one of the sulfate oxygen atoms). Most interestingly, Asp-145 in TMAO reductase (43) and Asp-147 in Me_2SO reductase (44) are at the same distance from the molybdenum ion as Glu-104 in YedY and have been proposed to function as a potential proton acceptor or donor in the catalytic mechanism (44). Finally, four aromatic residues, two tyrosine and two tryptophan residues (Tyr-47, Tyr-231, Trp-223, and Trp-246), constitute a hydrophobic pocket in the entrance leading to the active site of YedY,

TABLE II
YedYHis6 kinetic parameters

Note: No activity was observed for the tungsten substituted form of YedYHis6.

Substrate[a]	K_m	k_{cat}	k_{cat}/K_m
	mM	s^{-1}	$s^{-1}mM^{-1}$
Me_2SO	12.0	4.83	0.403
MetSO	119	25.6	0.215
TMSO	27.9	18.1	0.649
TMAO	22.0	19.0	0.864
TMAO (in 1 M urea)	46.4	14.8	0.319

[a] The abbreviations are as follows: Me_2SO, dimethyl sulfoxide; MetSO, L-methionine sulfoxide; TMSO, tetramethylene sulfoxide (tetrahydrothiophene 1-oxide).

similar to that for the architecturally distinct Me_2SO and TMAO reductases (43, 44). Two additional hydrophobic residues in YedY, Phe-203 and Val-103, are located within 5 Å of the molybdenum ion. Aromatic groups have been proposed previously to play a role in stacking and hydrophobic interactions with various cyclic substrates of oxidoreductase enzymes, and in YedY these conserved side chains are located at appropriate distances from the substrate binding cavity to play a similar role.

Activity of YedY in Solution—In order to better understand the function of YedY in *E. coli*, we have measured preliminary kinetic parameters using *in vitro* assays for both sulfite oxidases and reductases. To assess YedY activity as a sulfite oxidase, we used either *S. cerevisiae* cytochrome *c* (17) or ferricyanide (18) as an electron acceptor and followed the increase in absorbance at 550 and 420 nm, respectively. To monitor YedY activity as a reductase, a spectrophotometric assay was used to measure the substrate-dependent oxidation of BVH^+ (19). YedY did not show any detectable activity as a sulfite oxidase. In contrast, YedY functions as a reductase for substrates including TMAO, Me_2SO, phenylmethyl sulfoxide, methionine sulfoxide, and tetramethylene sulfoxide (Table II). However, unlike DmsABC reductase from *E. coli* (19), YedY is not able to reduce cyclic *N*-oxides such as pyridine *N*-oxide, nor more generic substrates for molybdopterin guanine dinucleotide-containing oxidoreductases, such as chlorate or hydroxylamine. Collectively, the substrate binding pocket features of YedY are in line with our finding that the enzyme could function as a reductase rather than a sulfite oxidase. We note that when the activity assays are run in the presence of 1 M urea (corresponding to concentrations found in the cryo-protectant solution used in our structure determination), there is little effect on k_{cat} in the reduction of TMAO, whereas K_m is increased 2-fold. Urea, observed bound to the active site in our YedY structure, is chemically similar to molecules such as Me_2SO and trimethylamine *N*-oxide, which are physiological substrates of Me_2SO and TMAO reductases, respectively, and in line with a possible role of urea as a weak substrate analogue inhibitor. Thus, despite the similar overall architecture of YedY and eukaryotic sulfite oxidases, our preliminary data on YedY suggest an entirely unique activity profile as a substrate-specific oxidoreductase, a finding that is in keeping with the specific catalytic residues we observe in the YedY active site.

Tungsten-substituted YedY—The atomic radii and chemical properties of tungsten are very similar to those of molybdenum (45). Stewart *et al.* (46) showed that dimethyl sulfoxide reductase from *Rhodobacter capsulatus* is capable of catalyzing the reduction of Me_2SO with either molybdenum or tungsten in the active site. Given the chemical similarities between molybdenum and tungsten, and the observation that both metals occur in enzymes ligated by the same pyranopterin (47), we explored the possibility of substituting tungsten for molybdenum in YedY.

Tungsten-substituted YedY was obtained by adding $Na_2O_4W{\cdot}2H_2O$ to the growth media to a final concentration of 10 mM. Tungsten-substituted YedY crystallized in the monoclinic $P2_1$ crystal form with 10 molecules per asymmetric unit forming two pentamers similar to that observed in the native crystal form. All subunits are similar with a range of root mean square deviations of 0.3–0.53 Å resulting from the pairwise superposition of 264 common C-α atoms. Moreover, the structure of tungsten YedY is very similar to the structure of native YedY with a range in root mean square deviation of 0.3- 0.6 Å resulting from the pairwise superposition of 264 common C-α atoms. All subunits have the pterin cofactor present, with the tungsten ion coordinated by three sulfur ligands. On the basis of their thermal parameters, all the cofactors can be refined with full occupancy, suggesting that tungsten-substituted pterin is fully incorporated into the protein.

The most striking difference between native YedY and tungsten YedY is the absence of the electron density corresponding to bound substrate/product in the active site adjacent to the metal ion (Fig. 5*B*). Instead, water molecules fill the active-site pocket, stabilized by hydrogen bonds to Tyr-47 (OH), Glu-104 (Oϵ1), and Tyr-231 (OH), similar to those formed to the urea in native YedY. The absence of bound ligand in the active site does not appear to greatly affect the nature of the substrate binding pocket with the majority of residues maintaining a highly similar conformation to that observed in native YedY. However, we do observe higher levels of disorder (as judged by higher temperature factors) in some regions of the active site in the tungsten substituted form, primarily at the far end of the cavity (Asp-229, Glu-230, and Arg-245).

Even though the tungsten-substituted YedY structure has been determined to higher resolution than that of native YedY (2.2 *versus* 2.5 Å), we also observe no electron density corresponding to the two putative oxo groups around the tungsten ion. Most intriguingly, our analysis of the tungsten-substituted form also shows a complete loss of reductase activity (Table II). This observation contrasts with those obtained from other reductase systems such as Me_2SO reductase from *R. capsulatus*, and TMAO reductase from *E. coli*, which have been shown to be equally or more active when tungsten is substituted for molybdenum (46, 48). The major difference between YedY and these enzymes is that the metal ion is coordinated by two pterin cofactors rather than one. This difference in coordination could account for the complete absence of catalytic activity for tungsten-substituted YedY, as it is believed that the cofactor(s) themselves directly modulate the reactivity and/or the reduction potential of the metal center in addition to having a role in electron transfer (1). No similar analysis of the tungsten-substituted forms of other single Moco enzymes (such as CSO) has been published. It will be interesting to verify if indeed the different coordination in these enzymes also results in inhibition by the tungsten ion.

A Novel Reductase with an Oxidase Fold—YedY, the catalytic subunit of the heterodimer oxidoreductase YedYZ from *E. coli*, is characterized by the presence of one molybdopterin-type cofactor and is not conjugated by an additional nucleotide. YedY and its orthologues are found in a wide variety of Gram-negative bacteria and share greater than 50% sequence identity. Our structural analysis indicates the residues involved in molybdopterin binding, in the metal coordination sphere, and in the substrate binding pocket are strictly conserved across the family of bacterial YedY-related proteins. In overall fold, YedY is most similar to that of the eukaryotic CSO (3), and our data further suggest the molybdenum cofactor is likely to have the same characteristics in both enzymes with two oxygen atoms as the fourth and fifth ligands of the metal ion. However, our preliminary kinetic data show that despite the overall "oxidase-like" architecture, YedY does not show detectable sulfite oxidase activity. These findings are in line with the structural details of the observed substrate binding pocket in our YedY structure. YedY lacks completely the positively charged binding pocket characteristic of sulfite binding in CSO (3), generated largely by three conserved arginine residues, and instead contains a conserved carboxylate and aromatic residues more in keeping with the active site of the architecturally distinct bacterial reductases (for *e.g.* Me_2SO and TMAO reductase). YedY and its orthologues thus represent a new type of membrane-anchored bacterial reductase widely present in Gram-negative bacteria. More generally, our work suggests the architecture found in the catalytically distinct and sequence-divergent eukaryotic sulfite oxidases, and the prokaryotic YedY-like reductases represent a much more commonly utilized molybdoenzyme scaffold than previously known.

Acknowledgments—We thank staff at Beamline 8.3.1 and 8.2.2 at the Advanced Light Source and the U. S. Department of Energy for access to the synchrotron radiation used in this study. We also thank Richard Pfuetzner for assistance with static light scattering and mass spectrometry analysis.

REFERENCES

1. Hille, R. (2002) *Trends Biochem. Sci.* **27,** 360–367
2. Enroth, C., Eger, B. T., Okamoto, K., Nishino, T., and Pai, E. F. (2000) *Proc. Natl. Acad. Sci. U. S. A.* **97,** 10723–10728
3. Kisker, C., Schindelin, H., Pacheco, A., Wehbi, W. A., Garrett, R. M., Rajagopalan, K. V., Enemark, J. H., and Rees, D. C. (1997) *Cell* **91,** 973–983
4. Schrader, N., Fischer, K., Theis, K., Mendel, R. R., Schwarz, G., and Kisker, C. (2003) *Structure* (*Lond.*) **11,** 1251–1263
5. Kappler, U., Bennett, B., Rethmeier, J., Schwarz, G., Deutzmann, R., McEwan, A. G., and Dahl, C. (2000) *J. Biol. Chem.* **275,** 13202–13212
6. Schindelin, H., Kisker, C., Hilton, J., Rajagopalan, K. V., and Rees, D. C. (1996) *Science* **272,** 1615–1621
7. Dias, J. M., Than, M. E., Humm, A., Huber, R., Bourenkov, G. P., Bartunik, H. D., Bursakov, S., Calvete, J., Caldeira, J., Carneiro, C., Moura, J. J., Moura, I., and Romao, M. J. (1999) *Struct. Fold Des.* **7,** 65–79
8. Boyington, J. C., Gladyshev, V. N., Khangulov, S. V., Stadtman, T. C., and Sun, P. D. (1997) *Science* **275,** 1305–1308
9. Ellis, P. J., Conrads, T., Hille, R., and Kuhn, P. (2001) *Structure* (*Lond.*) **9,** 125–132
10. Bertero, M. G., Rothery, R. A., Palak, M., Hou, C., Lim, D., Blasco, F., Weiner, J. H., and Strynadka, N. C. (2003) *Nat. Struct. Biol.* **10,** 681–687
11. Blattner, F. R., Plunkett, G., III, Bloch, C. A., Perna, N. T., Burland, V., Riley, M., Collado-Vides, J., Glasner, J. D., Rode, C. K., Mayhew, G. F., Gregor, J., Davis, N. W., Kirkpatrick, H. A., Goeden, M. A., Rose, D. J., Mau, B., and Shao, Y. (1997) *Science* **277,** 1453–1474
12. Sambrook, J., and Russel, D. W. (2001) *Molecular Cloning: A Laboratory Manual*, 3rd Ed., p. A2.4, Cold Spring Harbor Laboratory Press, Cold Spring Harbor, NY
13. Bilous, P. T., and Weiner, J. H. (1985) *J. Bacteriol.* **162,** 1151–1155
14. Benz, R., Boehler-Kohler, B. A., Dieterle, R., and Boos, W. (1978) *J. Bacteriol.* **135,** 1080–1090
15. Neu, H. C., and Heppel, L. A. (1965) *J. Biol. Chem.* **240,** 3685–3692
16. Lim, D., and Strynadka, N. C. (2002) *Nat. Struct. Biol.* **9,** 870–876
17. Cohen, H. J., and Fridovich, I. (1971) *J. Biol. Chem.* **246,** 359–366
18. Wilson, H. L., and Rajagopalan, K. V. (2004) *J. Biol. Chem.* **279,** 15105–15113
19. Simala-Grant, J. L., and Weiner, J. H. (1996) *Microbiology* **142,** 3231–3239
20. Otwinowski, Z., and Minor, W. (1997) *Methods Enzymol.* **276,** 307–325
21. Bailey, S. (1994) *Acta Crystallogr. Sect. D. Biol. Crystallogr.* **50,** 760–763
22. Weeks, C. M., and Miller, R. (1999) *J. Appl. Crystallogr.* **32,** 120–124
23. de La Fortelle, E., and Bricogne, G. (1997) *Methods Enzymol.* **276,** 472–479
24. Terwilliger, T. C., and Berendzen, J. (1999) *Acta Crystallogr. Sect. D. Biol. Crystallogr.* **55,** 849–861
25. Terwilliger, T. C. (2000) *Acta Crystallogr. Sect. D. Biol. Crystallogr.* **56,** 965–972
26. McRee, D. E. (1999) *J. Struct. Biol.* **125,** 156–165
27. Brünger, A. T., Adams, P. D., Clore, G. M., DeLano, W. L., Gros, P., Grosse-Kunstleve, R. W., Jiang, J. S., Kuszewski, J., Nilges, M., Pannu, N. S., Read, R. J., Rice, L. M., Simonson, T., and Warren, G. L. (1998) *Acta Crystallogr. Sect. D. Biol. Crystallogr.* **54,** 905–921
28. Laskowski, R. A., MacArthur, M. W., Moss, D. S., and Thornton, J. M. (1993) *J. Appl. Crystallogr.* **26,** 283–291
29. Sargent, F., Bogsch, E. G., Stanley, N. R., Wexler, M., Robinson, C., Berks, B. C., and Palmer, T. (1998) *EMBO J.* **17,** 3640–3650
30. Weiner, J. H., Bilous, P. T., Shaw, G. M., Lubitz, S. P., Frost, L., Thomas, G. H., Cole, J. A., and Turner, R. J. (1998) *Cell* **93,** 93–101
31. Drew, D., Sjostrand, D., Nilsson, J., Urbig, T., Chin, C. N., de Gier, J. W., and von Heijne, G. (2002) *Proc. Natl. Acad. Sci. U. S. A.* **99,** 2690–2695
32. Stewart, D. H., and Brudvig, G. W. (1998) *Biochim. Biophys. Acta* **1367,** 63–87
33. Romao, M. J., Archer, M., Moura, I., Moura, J. J., LeGall, J., Engh, R., Schneider, M., Hof, P., and Huber, R. (1995) *Science* **270,** 1170–1176

34. Holm, L., and Sander, C. (1995) *Trends Biochem. Sci.* **20,** 478–480
35. Janin, J., Miller, S., and Chothia, C. (1988) *J. Mol. Biol.* **204,** 155–164
36. Rebelo, J. M., Dias, J. M., Huber, R., Moura, J. J., and Romao, M. J. (2001) *J. Biol. Inorg. Chem.* **6,** 791–800
37. Dobbek, H., Gremer, L., Meyer, O., and Huber, R. (1999) *Proc. Natl. Acad. Sci. U. S. A.* **96,** 8884–8889
38. Truglio, J. J., Theis, K., Leimkuhler, S., Rappa, R., Rajagopalan, K. V., and Kisker, C. (2002) *Structure* (*Lond.*) **10,** 115–125
39. Johnson, J. L., Coyne, K. E., Garrett, R. M., Zabot, M. T., Dorche, C., Kisker, C., and Rajagopalan, K. V. (2002) *Hum. Mutat.* **20,** 74–79
40. Lam, C. W., Li, C. K., Lai, C. K., Tong, S. F., Chan, K. Y., Ng, G. S., Yuen, Y. P., Cheng, A. W., and Chan, Y. W. (2002) *Mol. Genet. Metab.* **75,** 91–95
41. Garrett, R. M., Johnson, J. L., Graf, T. N., Feigenbaum, A., and Rajagopalan, K. V. (1998) *Proc. Natl. Acad. Sci. U. S. A.* **95,** 6394–6398
42. Feng, C., Wilson, H. L., Hurley, J. K., Hazzard, J. T., Tollin, G., Rajagopalan, K. V., and Enemark, J. H. (2003) *Biochemistry* **42,** 12235–12242
43. Czjzek, M., Dos Santos, J. P., Pommier, J., Giordano, G., Mejean, V., and Haser, R. (1998) *J. Mol. Biol.* **284,** 435–447
44. Schneider, F., Lowe, J., Huber, R., Schindelin, H., Kisker, C., and Knablein, J. (1996) *J. Mol. Biol.* **263,** 53–69
45. Greenwood, N., and Earnshaw, A. (1984) *The Chemistry of the Elements*, p. 170, Pergamon Press Ltd., Oxford, UK
46. Stewart, L. J., Bailey, S., Bennett, B., Charnock, J. M., Garner, C. D., and McAlpine, A. S. (2000) *J. Mol. Biol.* **299,** 593–600
47. Stiefel, E. I., Coucouvanis, D., and Newton, W. E. (1993) *ACS Symposium, Series 535*, American Chemical Society, Washington, D. C.
48. Buc, J., Santini, C. L., Giordani, R., Czjzek, M., Wu, L. F., and Giordano, G. (1999) *Mol. Microbiol.* **32,** 159–168
49. Hutchinson, E. G., and Thornton, J. M. (1996) *Protein Sci.* **5,** 212–220
50. Kraulis, P. J. (1991) *Science* **254,** 581–582
51. DeLano, W. L. (2002) *The PyMol Molecular Graphics System*, DeLano Scientific, San Carlos, CA